Accepted Manuscript

Adsorption and reaction mechanism of arsenic vapors over γ-Al_2O_3 in the simulated flue gas containing acid gases

Hongyun Hu, Dunkui Chen, Huan Liu, Yuhan Yang, Hexun Cai, Junhao Shen, Hong Yao

PII: S0045-6535(17)30489-7

DOI: 10.1016/j.chemosphere.2017.03.114

Reference: CHEM 19032

To appear in: *ECSN*

Received Date: 4 November 2016

Revised Date: 24 March 2017

Accepted Date: 27 March 2017

Please cite this article as: Hu, H., Chen, D., Liu, H., Yang, Y., Cai, H., Shen, J., Yao, H., Adsorption and reaction mechanism of arsenic vapors over γ-Al_2O_3 in the simulated flue gas containing acid gases, *Chemosphere* (2017), doi: 10.1016/j.chemosphere.2017.03.114.

Graphical abstract

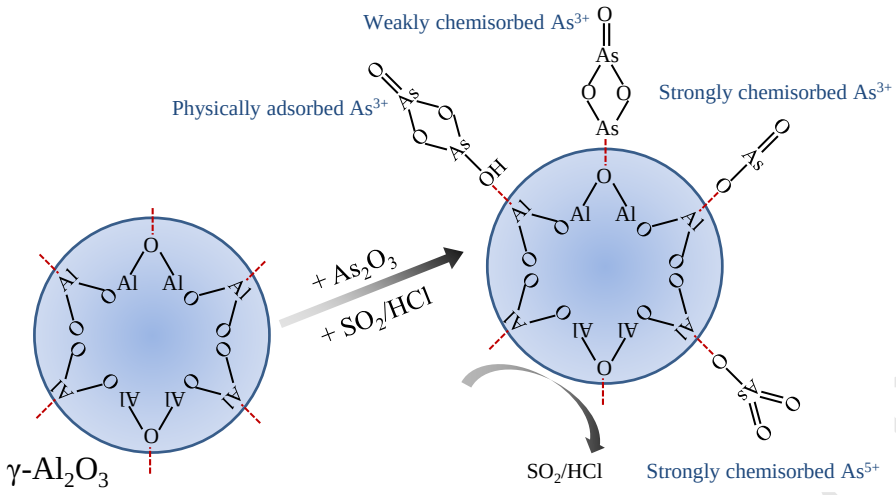

Adsorption and reaction mechanism of arsenic vapors over γ-Al_2O_3 in the simulated flue gas containing acid gases

Hongyun Hu[a], Dunkui Chen[a], Huan Liu[a,b], Yuhan Yang[a], Hexun Cai[a], Junhao Shen[a], Hong Yao [a,b,*]

[a] *State Key Laboratory of Coal Combustion, School of Energy and Power Engineering, Huazhong University of Science and Technology, Wuhan 430074, China*

[b] *Department of New Energy Science and Engineering, School of Energy and Power Engineering, Huazhong University of Science and Technology, Wuhan 430074, China*

[*] Correspondingauthor.Tel & Fax: +86-27-87545526(O)

E-mail: hyao@mail.hust.edu.cn (Prof. Hong Yao)

Abstract

Arsenic emission from fuel combustion and metal smelting flue gas causes serious pollution. Addition of sorbents is a promising way for the arsenic capture from high temperature flue gas. However, it is difficult to remove arsenic from SO_2/HCl-rich flue gas due to the competitive reaction of the sorbents with arsenic and these acid gases. To solve this problem, arsenic adsorption over γ-Al_2O_3 was studied in this work to evaluate its adsorption mechanism, resistance to acid gases as well as regeneration behavior. The results show that γ-Al_2O_3 had good resistance to acid gases and the arsenic adsorption by γ-Al_2O_3 could be effectively carried out at a wide temperature range between 573 and 1023 K. Nevertheless, adsorption at higher-temperature (like 1173 K) leaded to the decrease of surface area and the rearrangement of crystal structure of γ-Al_2O_3, reducing the active sites for arsenic adsorption. The adsorption of arsenic was confirmed to occur at different active sites in γ-Al_2O_3 by forming various adsorbed species. Increasing temperature facilitated arsenic transformation into more stable chemisorbed As^{3+} and As^{5+} which were difficult to remove through thermal treatment regeneration. Fortunately, the regeneration of spent γ-Al_2O_3 could be well performed using NaOH solution.

Keywords: Arsenic adsorption; γ-Al_2O_3; Acid gases; Species; Regeneration

1. Introduction

Arsenic is extremely toxic and the release of arsenic has raised great environmental concerns (Sarkar and Paul, 2016). Nowadays, positive measures have been taken in China to strictly control the arsenic emission, especially for the major arsenic-emitting industries, like fuel combustion and metal smelting (He et al., 2013). Due to the high volatilization, arsenic is predominantly evaporated into the high temperature flue gas in the form of vapor-phases (such as As_2O_3) (Bashaa et al., 2008; Shen et al., 2015). Arsenic vapors tend to be enriched in fine particles as temperature decreased in the cooling process of the flue gas, which is difficult to captured by normally used air pollution control devices (Hu et al., 2016; Liu et al., 2016). On the other hand, the presence of arsenic in the flue gas has negative effect for the recovery of SO_2 in the metal smelting (Dalewski, 1999). Moreover, it may also cause the deactivation of the catalysts of the widely used selective catalytic reduction system for NO_x control (Hu et al., 2016). Therefore, it's essential for the capture of arsenic vapors from the high temperature flue gas.

Previous literatures, including our research, have demonstrated that interactions between arsenic vapors and Al, Ca and/or Fe-compounds enhanced arsenic stabilization in coarse particles, increasing arsenic trapping efficiency (Hu et al., 2015; Zhang et al., 2016). Thus, it provides a promising way for arsenic capture from the flue gas through the addition of Al, Ca and/or Fe-based sorbents. Usually, arsenic is coexisted with sulfur in most of coals and metal minerals (Shen et al., 2015; Lattanzi et al., 2008). As a result, arsenic-rich flue gas probably contains a high concentration

of SO_2. Among the arsenic capture sorbents, CaO was widely investigated and showed good capacity for the adsorption of arsenic vapors (Li et al., 2007; Tian et al., 2016). However, CaO had low resistance to SO_2, and arsenic sorption was strongly suppressed by the reaction of SO_2 with CaO (Seams and Wendt, 2007; Chen et al., 2015). So far, it is still a challenge to find more effective and suitable sorbents for the adsorption of arsenic at the presence of SO_2.

Comparing with CaO, active alumina has large surface area and proper pore structures. Using of active alumina for the arsenic sorption from liquids has been successfully carried out (Han et al., 2013; Önnbya et al., 2014). Several studies have also confirmed that arsenic could be captured from the high temperature flue gas by alumina (Contreras et al., 2009; Luo et al., 2011). However, the adsorption of arsenic under the influence of acid gases had been scarcely investigated. Comparing with CaO, alumina contained stronger surface acid sites and weaker basic sites (Zhao et al., 2011). Based on this, alumina might show better resistance to acid gases than CaO although the adsorption of SO_2 by alumina at low temperatures was observed (Xie et al., 2014). In addition to the adsorption atmosphere, the sorption behavior was generally determined by the reaction temperature (Ninomiya et al., 2009; Wang et al., 2013). The change of the operating temperature might alter the pathway for the adsorption of SO_2 as well as arsenic vapors. In view of these points, the present study observe the arsenic adsorption by alumina under the influence of acid gases at various temperatures, and the mechanism regarding the arsenic adsorption and reaction over alumina was clarified.

In particular, arsenic adsorption mechanism on active alumina (γ-Al_2O_3) was studied at temperatures ranging from 573 K to 1323 K. The experiments were conducted in the simulated flue gas containing arsenic vapors within/without acid gases (SO_2/HCl). The differences in arsenic sorption capacity were discussed considering the effects of adsorption temperature and the presence of acid gases in the flue gas. To further understand the mechanism regarding the arsenic adsorption, the species of the arsenic captured on the alumina were determined. For the recycling of the γ-Al_2O_3, regeneration of the spent alumina was carried out through both thermal treatment and NaOH solution leaching process.

2. Experimental procedures

2.1 Materials

Synthetic γ-Al_2O_3 used in this work was purchased from Aladdin (shanghai, China). Before experiments, the alumina particles were carefully sieved and the size fraction between 200 and 300 μm was selected. To provide constant arsenic vapors, arsenic was firstly transformed into AsH_3(g) by using a hydride generator and then was oxidized to form arsenic vapors at 973 K (as shown in Fig. SM-1 in Supplementary Material (SM)). In the hydride generator, AsH_3(g) was produced by mixing of $NaAsO_2$ solution (dissolved in 1 v/v% HCl solution), HCl solution and KBH_4 solution. The concentration of AsH_3(g) was constantly maintained through the precise control of the $NaAsO_2$ solution flow rate using a peristaltic pump. Thereafter, the produced AsH_3(g) was carried by pure argon to mix with N_2, O_2 and acid gases (SO_2 and HCl) before entering the reactor. All the reagents used here are of high

purity grade.

2.2 Adsorption Experiments

Fig. SM-1 illustrates the schematic diagram of arsenic adsorption system. The system mainly consisted of two parts, including a mixing reactor for AsH_3(g) production and a two-stage reactor for AsH_3(g) oxidation and arsenic vapors adsorption. Firstly, the simulated flue gas with AsH_3(g) was prepared as stated before. The flue gas was heated at 973 K in the first stage of the two-stage reactor. After the oxidation of AsH_3(g), the simulated flue gas was measured, comprising 86 v/v% N_2, 6 v/v% O_2 and 8 v/v% H_2O(g) and 200ppm As_2O_3(g). In the case of observing the effects of acid gases on the arsenic adsorption, the SO_2 or HCl was input into the reactor and the concentration was kept at 2000ppm and 500ppm, respectively.

Secondly, the simulated flue gas was sent to the second stage of the two-stage reactor and the adsorption of arsenic vapors was conducted at temperatures ranging from 573 to 1323 K. Before arsenic adsorption, a certain amount of γ-Al_2O_3 was placed in the sorbent holder and was preheated in the flue gas without As_2O_3(g). Then, the hydride generator was operated and the arsenic vapors were present in the simulated flue gas. The reactions between γ-Al_2O_3 and the simulated flue gas compositions were taken place in the sorbent holder and the details of the sorbent holder were explained elsewhere (Chen et al., 2015).

Finally, the reacted alumina after adsorption was cooled to the room temperature in the arsenic free flue gas, after which the products were collected for the subsequent analysis. The observation of arsenic sorption capacity for high-temperature treated

117 alumina as well as regenerated alumina was carried out in the same way as for the raw
118 γ-Al_2O_3.

119 **2.3 Regeneration of spent alumina**

120 The regeneration of spent alumina was tried by using two methods in this study.
121 On one hand, the adsorbed arsenic was removed from the spent alumina through
122 thermal treatment in arsenic-free atmosphere. The spent alumina products obtained at
123 low temperatures from 573 to 1023 K were tested, which were sent to heat at 1173 K
124 for 10 min in N_2 or air atmosphere.

125 On the other hand, the regeneration of the spent alumina was carried out by
126 immersing the used sorbents in diluted NaOH solution at 298 and 348 K, respectively.
127 The regenerated alumina was washed by deionized water and dried at 378 K. The
128 performance of the NaOH-treated alumina for arsenic capture was tested at 573 K for
129 7 cycles.

130 **2.4 Analytical methods**

131 The adsorbed arsenic in the reacted alumina was leached out by 20 v/v% HCl
132 solution and determined by atomic fluorescence spectroscopy (AFS). Besides, the
133 speciation of the adsorbed arsenic was measured by using AFS coupled with high
134 performance liquid chromatography (HPLC). Before the speciation detection, arsenic
135 should be also transformed into solution by using 0.5 mol/L phosphoric acid as
136 leaching solution. The leached various forms of arsenic (arsenite (As^{3+}) and arsenate
137 (As^{5+})) were separated in the analytical column (Hamilton PRP-X100) and the
138 concentration of each species of arsenic was determined by AFS. Each experiment

was repeated for several times to make sure the results believable. To compare the arsenic adsorption capacity in the flue gas with and without acid gases, a difference ratio (β) was defined and calculated as Ep. (1).

$$\beta = \frac{\mathrm{m2} - \mathrm{m1}}{\mathrm{m1}} \times 100\% \qquad (1)$$

where, m1 means arsenic capture capacity in the flue gas without SO_2/HCl, mg/g sorbent, m2 means arsenic capture capacity in the flue gas with SO_2/HCl, mg/g sorbent.

The properties of the activated alumina before and after arsenic adsorption were comparatively observed. X-ray powder diffraction (XRD, X'Pert PRO, PANalytical B.V.) was applied to analyze the crystalline structure change of the alumina. The measurement of BET specific surface area was conducted via N_2 isothermal adsorption (Micromeritics ASPS 2020).

3. Results and Discussion

3.1 Effects of acid gases on the arsenic adsorption by γ-Al_2O_3

Fig. 1 presents the arsenic adsorption by γ-Al_2O_3 in the flue gas with and without SO_2 at a retention time of 5 min. The results showed that γ-Al_2O_3 showed good resistance to SO_2 at each temperature from 573 to 1323 K. Compared with CaO (Chen et al., 2015), the presence of SO_2 in the simulated flue gas had little impact on the arsenic capture by γ-Al_2O_3. It might be attributed to the large surface area of γ-Al_2O_3. γ-Al_2O_3 could offer enough active sites for the adsorption for both As_2O_3 and SO_2 in the short reaction time.

To further confirm the suspicion, γ-Al_2O_3 was exposed in the arsenic-containing

flue gas for longer retention time. The difference ratios (as defined in section 2.2) regarding the arsenic adsorption at the absence or presence of SO_2 were displayed in Fig. 2. The presence of SO_2 generally had a negative effect on the arsenic adsorption, which became remarkable with the retention time increasing from 5 to 90 min. It was probable that the adsorption of both As_2O_3 and SO_2 was taken place in the same active site of γ-Al_2O_3. The active sites were gradually occupied in the long-time adsorption process. The lack of active sites leaded to the competitive adsorption of As_2O_3 and SO_2 over γ-Al_2O_3. As a result, the adsorption capacity of arsenic was reduced. Even so, γ-Al_2O_3 had much better resistance to SO_2 than CaO.

Similarly, the effect of HCl on the arsenic adsorption over γ-Al_2O_3 was observed. The experiments were performed in 5 min and the results (shown in Fig. SM-2) compared the effect of HCl on CaO and γ-Al_2O_3 for the adsorption of arsenic. From the results, arsenic capture by CaO was strongly affected by HCl while the capture of arsenic by γ-Al_2O_3 was slightly affected. Moreover, the effect of HCl showed different tendencies at various temperatures for both CaO and γ-Al_2O_3. The adsorption of HCl by CaO was mainly through the chemisorption (Tongamp et al., 2009) which was enhanced with the temperature increasing from 573 K to 1023 K. Therefore, the adsorption of arsenic by CaO was greatly suppressed at 1023 K. However, the presence of HCl had little impact or even positive effect on the arsenic adsorption by CaO at higher temperatures. It was widely observed that CaO particles were easily sintered at high temperatures (Liu et al., 2010; Hu et al., 2013). The surface characteristics of the sintering CaO particles might be improved under the

182 influence of HCl, increasing the capture capacity of CaO (Wu et al., 2014). In contrast,
183 the adsorption of HCl on the surface of γ-Al_2O_3 was mainly through the physical
184 adsorption (Vigue et al., 1998), which was effective at 573 K. The acidity of HCl was
185 stronger than that of SO_2 and the adsorption of HCl on the surface of γ-Al_2O_3 is not
186 conductive to the capture of arsenic. Nevertheless, the physical sorption of HCl was
187 inhibited at high temperatures and the effect of HCl became progressively smaller
188 with the increase of the adsorption temperatures.

189 On the other hand, an interesting phenomena was found in Fig. 1. Unlike CaO,
190 the capacity of γ-Al_2O_3 for the arsenic adsorption was almost the same at
191 temperatures from 573 to 1023 K. It was attractive especially for the effective arsenic
192 capture at low temperatures. However, arsenic adsorption was partly suppressed at
193 1173 and 1323 K and the similar phenomena was also found for the arsenic capture by
194 CaO (Chen et al., 2015). Compared with CaO, arsenic capture by γ-Al_2O_3 was less
195 affected at high temperatures and the mechanism of As_2O_3(g) adsorption over γ-Al_2O_3
196 should be further addressed.

197 **3.2 Mechanism of As_2O_3(g) adsorption over γ-Al_2O_3**

198 Fig. 3 depicts the arsenic adsorption capacity over γ-Al_2O_3 at various retention
199 time as a function of temperature. From the results, the increase of retention time had
200 few effect on the arsenic adsorption at temperatures between 573 K and 1023 K.
201 However, arsenic adsorption at higher temperatures was strongly affected by the
202 retention time. The adsorption capacity was remarkably decreased at 1173 and 1323 K
203 with the increasing of the retention time from 1 min to 10 min. The inhabitation of

arsenic adsorption at high temperature was further confirmed by determining arsenic adsorption over thermally treated Al_2O_3 (shown in Table SM-1). The adsorption capacity was sharply decreased after heating Al_2O_3 for 10 min and longer time. In contrast, the adsorption capacity was hardly affected when γ-Al_2O_3 was heated at 573 K and 873 K even for 60 min (not shown here).

Generally, γ-Al_2O_3 is one kind of the metastable "transition" alumina structural polymorphs which is unstable during high temperature treatment (Busca, 2014). As shown in Table SM-2, the specific surface area of γ-Al_2O_3 particles was reduced in the high temperature adsorption process. In detail, few changes in the specific surface area were found as Al_2O_3 heated at 1023 K. However, large decrease in specific surface area was observed for samples as the adsorption temperature was raised to 1173 and 1323 K. On the other hand, the chemical phase of the Al_2O_3 was changed at these high temperatures. Fig. SM-3 shows the XRD patterns of the alumina heated at 1273 K as a function of heating time. The presence of new diffraction peaks (such as at 2θ values of 31.8° and 32.9°) revealed that Al_2O_3 was structurally rearranged in the high temperature adsorption process. Specifically, γ-Al_2O_3 was transformed to θ-Al_2O_3 in the heating process as supported by previous studies (Kwak et al., 2011). Based on preliminary analysis, the inhabitation of arsenic adsorption at high temperatures was attributed to the change of the physical characteristics as well as the crystal structure of Al_2O_3. The decrease of specific surface area might lead to few active sites available for the adsorption of arsenic. And the structural rearrangements of γ-Al_2O_3 was supposed to change the adsorption sites for arsenic.

To clarify the pathway for arsenic adsorption over γ-Al_2O_3, detailed studies were carried out to identify the speciation of the captured arsenic (from the flue gas with and without SO_2). The distribution of As^{3+} fraction in the reaction products were listed in Table 1 and the rest of arsenic was in the form of As^{5+}. Arsenic was predominantly in the form of As^{3+} in the reaction products obtained at temperatures from 573 K to 873 K. Increasing of the adsorption temperature favored arsenic capture in the form of arsenates (As^{5+}). The presence of SO_2 in the flue gas slightly affected the pathway for arsenic adsorption over Al_2O_3, which tended to facilitate arsenic distribution in the form of As^{3+}.

Like the adsorption of SO_2 (Zhao et al., 2012), arsenic adsorption could take place at different active sites over γ-Al_2O_3 by forming various adsorbed species. Fig. SM-4 gives several possible model of adsorbed arsenic species. At low temperature like 573 K, the interactions of γ-Al_2O_3 and moisture resulted in the formation of hydroxyl groups (•OH). Then arsenic vapors could be adsorbed on these groups by forming physically adsorbed species (Fig. SM-4(a)). Meanwhile, arsenic could be captured to form weakly chemisorbed species (Fig. SM-4(b)). Increasing temperature enhanced the strongly chemisorption of arsenic both in the form of As^{3+} and As^{5+} (Fig. SM-4(c) and (d)), which probably had good thermal stability. These speculations were consistent with the results regarding the detection of the adsorbed arsenic's stabilities which were discussed in section 3.3.

3.3 Regeneration of spent γ-Al_2O_3

As stated before, a large fraction of arsenic might be adsorbed through physical

adsorption at low temperatures in the form of As^{3+}. The removal of physically adsorbed species from sorbents was usually proposed by using thermal treatment method (Yang et al., 2014; Hamzehlouyan et al., 2016). Based on this, the removal of arsenic from the reacted Al_2O_3 was conducted at 1173 K in arsenic-free atmosphere (air and N_2, respectively). Both of the removal efficiency of arsenic and the speciation of the remained arsenic was observed. As shown in Fig. 4, the removal efficiency differed in the products obtained at various adsorption temperatures. More arsenic was released from the reacted Al_2O_3 obtained at low temperatures like 573 and 723 K. Arsenic adsorbed at high temperatures was difficult to release. Compared with arsenic removal in N_2, more arsenic was stabilized in the Al_2O_3 by forming As^{5+} under air atmosphere.

The discrepancy in thermal stability of the captured arsenic further confirmed the presence of various species of the adsorbed arsenic over Al_2O_3. The high fraction of released arsenic for products obtained at 573 K and 723 K suggested that arsenic adsorption was mainly through physically adsorption and weakly chemisorption at low temperature. The As^{3+} in the products obtained at high temperatures was assigned to the strongly chemisorbed As^{3+} which could be well stabilized even heated at 1173 K. The strongly chemisorbed As^{5+} generally stable at the experimental temperature as evident from the large fraction of remained arsenic in the form of As^{5+}.

Considering the poor removal efficiency of captured arsenic during thermal treatment, the regeneration of spent γ-Al_2O_3 was tried through the leaching process of NaOH solution. After regeneration, the γ-Al_2O_3 was exposed in the simulated flue gas

for the adsorption of arsenic at 573 K for several recycles. The results in Fig. 5 indicated that the regeneration of γ-Al_2O_3 was effectively conducted by using alkaline solution leaching. In contrast, operation at 348 K showed a better performance than that at 298 K in the subsequent cycling experiments.

The regeneration temperature could affect the extraction of arsenic from the reacted γ-Al_2O_3. As shown in Table 2, regeneration at 348 K could maintain a high extraction fraction of arsenic. Less arsenic was extracted at 298 K and the extraction fraction was further decreased with the increasing of regeneration cycles. As a result, more arsenic was remained in the regenerated γ-Al_2O_3 and less active sites were left for the adsorption of arsenic. The regeneration at 348 K enhanced the interaction between NaOH solution and γ-Al_2O_3, promoting the arsenic extraction. The similar phenomena was found for the regeneration of spent magnetic nanomaterials for arsenic removal from liquids (Zhang et al., 2010). However, the regeneration by using NaOH solution probably increased the surface basic sites of γ-Al_2O_3, which might reduce the resistance to acid gases. It's essential to comprehensively evaluate the properties of the regenerated γ-Al_2O_3 by using alkaline solution.

4. Conclusions

The mechanism were illuminated regarding the arsenic adsorption over γ-Al_2O_3 in the simulated flue gas containing acid gases. γ-Al_2O_3 showed good performance for the adsorption of arsenic at a wide temperature range from 573 to 1023 K which was hardly affected at the presence of acid gases in a certain retention time. However, in the long-time adsorption process, acid gases competed with arsenic vapors to react

292 with γ-Al_2O_3, suppressing the adsorption of arsenic. The high temperature adsorption
293 was also not conductive for the arsenic adsorption due to the damage of the pore
294 structure as well as the rearrangement of the crystal structure of γ-Al_2O_3.

295 The adsorption of arsenic over γ-Al_2O_3 was a complicated process with arsenic
296 adsorbed at various active sites in γ-Al_2O_3. The formation of different arsenic species
297 was confirmed which showed various thermal stability. Although the arsenic capacity
298 was almost the same as adsorption conducted at temperatures from 573 to 1023 K, the
299 increasing of adsorption temperature enhanced the arsenic transformation into more
300 stable chemisorbed As^{3+} and As^{5+}. Moreover, the spent γ-Al_2O_3 was successfully
301 regenerated through the leaching process by NaOH solution. The regenerated γ-Al_2O_3
302 at 348 K showed good performance for the arsenic adsorption for reclycling for 7
303 times.

304 **Acknowledgments**

305 This work was funded by the National Natural Science Foundation of China
306 (51606075, 51506064) and General Financial Grant from the China Postdoctoral
307 Science Foundation (Grant, 2016M592330). The authors are grateful to the Analytical
308 and Testing Center of Huazhong University of Science and Technology for the
309 experimental measurements.

310 **References**

311 Bashaa, C.A., Selvi, S.J., Ramasamy, E., Chellammal, S., 2008. Removal of arsenic
312 and sulphate from the copper smelting industrial effluent. Chem. Eng. J. 141, 89-98.

313 Busca, G., 2014. The surface of transitional aluminas: A critical review. Catal. Today
314 226, 2-13.

315 Chen, D.K., Hu, H.Y., Xu, Z., Liu, H., Cao, J.X., Shen, J.H., Yao, H., 2015. Findings
316 of proper temperatures for arsenic capture by CaO in the simulated flue gas with and
317 without SO_2. Chem. Eng. J. 267, 201-206.

318 Contreras, M.L., Arostegui, J.M., Armesto, L., 2009. Arsenic interactions during
319 co-combustion processes based on thermodynamic equilibrium calculations. Fuel 88,
320 539-546.

321 Dalewski, F., 1999. Removing arsenic from copper smelter gases. JOM. 51, 24-26.

322 Hamzehlouyan, T., Sampara, C.S., Li, J.H., Kumar, A., Epling, W.S., 2016. Kinetic
323 study of adsorption and desorption of SO_2 over γ-Al_2O_3 and Pt/γ-Al_2O_3. Appl. Catal.
324 B: Environ. 181, 587-598.

325 Han, C.Y., Li, H.Y., Pu, H.P., Yu, H.L., Deng, L., Huang, S., Luo, Y.M., 2013.
326 Synthesis and characterization of mesoporous alumina and their performances for
327 removing arsenic(V). Chem. Eng. J. 217, 1-9.

328 He, B., Yun, Z.J., Shi, J.B., Jiang, G.B., 2013. Research progress of heavy metal
329 pollution in China: Sources, analytical methods, status, and toxicity. Chin. Sci. Bull.
330 58, 134-140.

331 Hu, H.Y., Liu, H., Chen, J., Li, A.J., Yao, H., Low, F., Zhang, L.A., 2015. Speciation
332 transformation of arsenic during municipal solid waste incineration. P. Combust. Inst.
333 35, 2883-2890.

334 Hu, H.Y., Liu, H., Shen, W.Q., Luo, G.Q., Li, A.J., Lu, Z.L., Yao, H., 2013.
335 Comparison of CaO's effect on the fate of heavy metals during thermal treatment of
336 two typical types of MSWI fly ashes in China. Chemosphere 93, 590-596.

337 Hu, W.S., Gao, X., Deng, Y.W., Qu, R.Y., Zheng, C.H., Zhu, X.B., Cen, K.F., 2016.
338 Deactivation mechanism of arsenic and resistance effect of SO_4^{2-} on commercial
339 catalysts for selective catalytic reduction of NO_x with NH_3. Chem. Eng. J. 293,
340 118-128.

341 Kwak, J.H., Peden, C.H.F., Szanyi, J., 2011. Using a surface-sensitive chemical probe
342 and a bulk structure technique to monitor the γ-to θ-Al_2O_3 phase transformation. J.
343 Phys. Chem. C 115, 12575-12579.

344 Lattanzi, P., Pelo, S.D., Musu, E., Atzei, D., Elsener, B., Fantauzzi, M., Rossi, A.,
345 2008. Enargite oxidation: A review. Earth-Sci. Rev. 86, 62-88.

346 Li, Y.Z., Tong, H.L., Zhuo, Y.Q., Li, Y., Xu, X.C., 2007. Simultaneous removal of
347 SO_2 and trace As_2O_3 from flue gas: Mechanism, kinetics study, and effect of main
348 gases on arsenic capture. Environ. Sci. Technol. 41, 2894-2900.

349 Liu, G.L., Cai, Y., Hernandez, D., Schrlau, J., Allen, M., 2016. Mobility and
350 speciation of arsenic in the coal fly ashes collected from the Savannah River Site
351 (SRS). Chemosphere 151, 138-144.

352 Liu, W.Q., Feng, B., Wu, Y.Q., Wang, G.X., Barry, J., Costa, J.C., 2010. Synthesis of
353 sintering-resistant sorbents for CO_2 capture. Environ. Sci. Technol. 44, 3093-3097.

354 Luo, Y., Giammar, D.E., Huhmann, B.L., Catalano, J.G., 2011. Speciation of
355 selenium, arsenic, and zinc in class C fly ash. Energy Fuel 25, 2980-2987.

356 Ninomiya, Y., Wang, Q.Y., Xu, S.Y., Mizuno, K., Awaya, I., 2009. Effect of
357 additives on the reduction of $PM_{2.5}$ emissions during pulverized coal combustion.
358 Energy Fuel 23, 3412-3417.

359 Önnbya, L., Kumar, P.S., Sigfridsson, K.G.V., Wendt, O.F., Carlson, S., Kirsebom,
360 H., 2014. Improved arsenic(III) adsorption by Al_2O_3 nanoparticles and H_2O_2:
361 Evidence of oxidation to arsenic(V) from X-ray absorption spectroscopy.
362 Chemosphere 113, 151-157.

363 Sarkar, A., Paul, B., 2016. The global menace of arsenic and its conventional
364 remediation - A critical review. Chemosphere 158, 37-49.

365 Seames, W.S., Wendt, J.O.L., 2007. Regimes of association of arsenic and selenium
366 during pulverized coal combustion. P. Combust. Inst. 31, 2839-2846.

367 Shen, F.H., Liu, J., Zhang, Z., Dai, J.X., 2015. On-line analysis and kinetic behavior
368 of arsenic release during coal combustion and pyrolysis. Environ. Sci. Technol. 49,
369 13716-13723.

370 Tian, C., Gupta, R., Zhao, Y.C., Zhang, J.Y., 2016. Release behaviors of arsenic in
371 fine particles generated from a typical high-arsenic coal at a high temperature. Energy
372 Fuel, 30, 6201-6209.

373 Tongamp, W., Zhang, Q.W., Shoko, M., Saito, F., 2009. Generation of hydrogen from
374 polyvinyl chloride by milling and heating with CaO and $Ni(OH)_2$. J. Hazard. Mater.
375 167, 1002-1006.

376 Vigue, Â, H., Quintard, P., Merle-MeÂjean, T., Lorenzelli, V., 1998. An FT-IR Study
377 of the chlorination of γ-alumina surfaces. J. Eur. Ceram. Soc. 18, 305-309.

378 Wang, X.Y., Huang, Y.J., Zhong, Z.P., Yan, Y.P., Niu, M.M., Wang, Y.X., 2013.
379 Control of inhalable particulate lead emission from incinerator using kaolin in two
380 addition modes. Fuel Process. Technol. 119, 228-235.

381 Wu, X.M., Yu, Y.S., Zhang, C.Y., Wang, G.X., Feng, B., 2014. Identifying the CO_2
382 capture performance of $CaCl_2$-supported amine adsorbent by the improved field
383 synergy theory. Ind. Eng. Chem. Res. 53, 10225-10237.

384 Xie, Y., Chen, Y., Ma, Y.G., Jin, Z.L., 2011. Investigation of simultaneous adsorption
385 of SO_2 and NO on γ-alumina at low temperature using DRIFTS. J. Hazard. Mater. 195,
386 223-229.

387 Yang, J.P., Zhao, Y.C., Zhang, J.Y., Zheng, C.G., 2014. Regenerable cobalt oxide
388 loaded magnetosphere catalyst from fly ash for mercury removal in coal combustion
389 flue gas. Environ. Sci. Technol. 48, 14837-14843.

390 Zhang, S.X., Niu, H.Y., Cai, Y.Q., Zhao, X.L., Shi, Y.L., 2010. Arsenite and arsenate
391 adsorption on coprecipitated bimetal oxide magnetic nanomaterials: $MnFe_2O_4$ and
392 $CoFe_2O_4$. Chem. Eng. J. 158, 599-607.

393 Zhang, Y., Wang, C.B., Liu, H.M., 2016. Experiment and mechanism research on
394 gas-phase As_2O_3 adsorption of Fe_2O_3/γ-Al_2O_3. Fuel 181, 1034-1040.

395 Zhao, L., Li, X.Y., Hao, C., Raston, C.L., 2012. SO_2 adsorption and transformation on
396 calcined NiAl hydrotalcite-like compounds surfaces: An in situ FTIR and DFT study.
397 Appl. Catal. B: Environ. 117-118, 339-345.

398 Zhao, L., Li, X.Y., Quan, X., Chen, G.H., 2011. Effects of surface features on sulfur
399 dioxide adsorption on calcined NiAl hydrotalcite-like compounds. Environ. Sci.
400 Technol. 45, 5373-5379.

Tables list

Table 1 Distribution of As^{3+} fraction (%) in the reaction products obtained from the simulated flue gas with and without SO_2

Flue gas characteristic	573 K	723 K	873 K	1023 K	1173 K	1323 K
Without SO_2	100	87.21	83.62	47.48	19.4	0
Within SO_2	93.0	94.47	91.47	58.26	19.5	3.65

Table 2 Extraction fraction (%) of arsenic from the reaction products after multiple cycles of adsorption

Extracting temperature	Number of cycle					
	1	2	3	4	5	6
298 K	63.4	45.7	35.3	28.1	25.4	22.3
348 K	87.6	90.1	85.2	83.9	85.3	81.1

Figure captions

Fig. 1. Arsenic adsorption capacity by alumina in the flue gas with/without SO_2 at temperatures from 573 to 1323 K

Fig. 2. The difference ratio of arsenic capture in the simulated flue gas with/without SO_2 at various retention time

Fig. 3. Arsenic adsorption capacity by alumina at temperatures from 573 to 1323 K

Fig. 4. Arsenic distribution in the reaction products after thermal treatment at 1173 K (Left column for treatment in air and right column for treatment in N_2)

Fig.5. Multiple cycles of arsenic adsorption by alumina regenerated at various temperatures

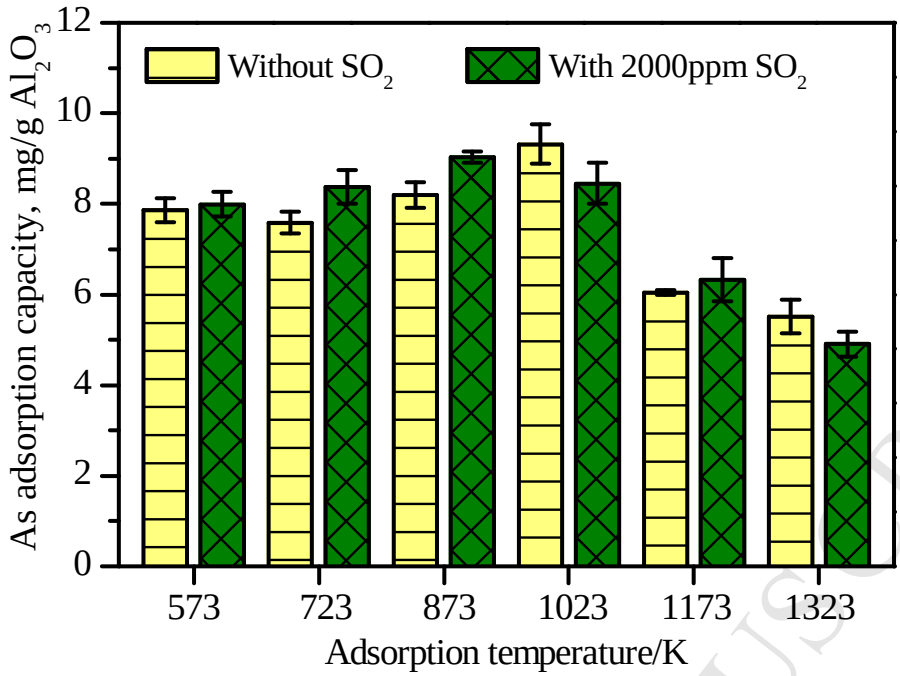

Fig. 1. Arsenic adsorption capacity by alumina in the flue gas with/without SO_2 at temperatures from 573 to 1323 K

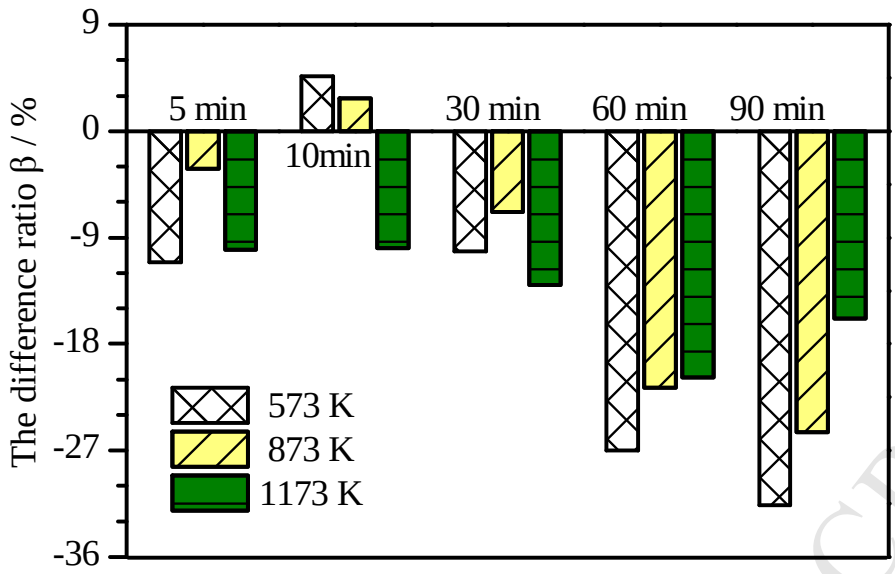

Fig. 2. The difference ratio of arsenic capture in the simulated flue gas with/without SO_2 at various retention time

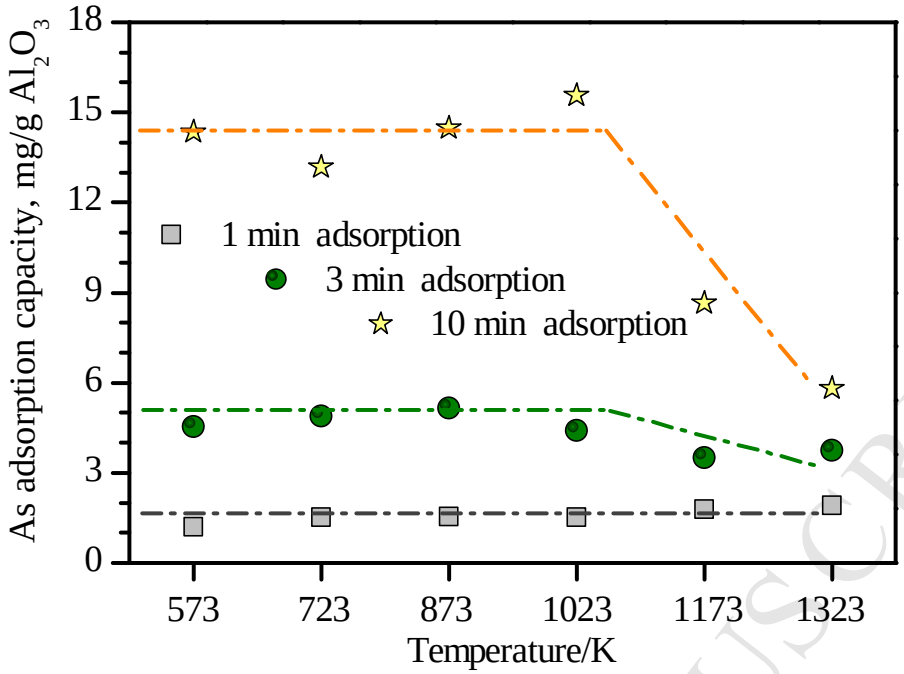

Fig. 3. Arsenic adsorption capacity by alumina at temperatures from 573 to 1323 K

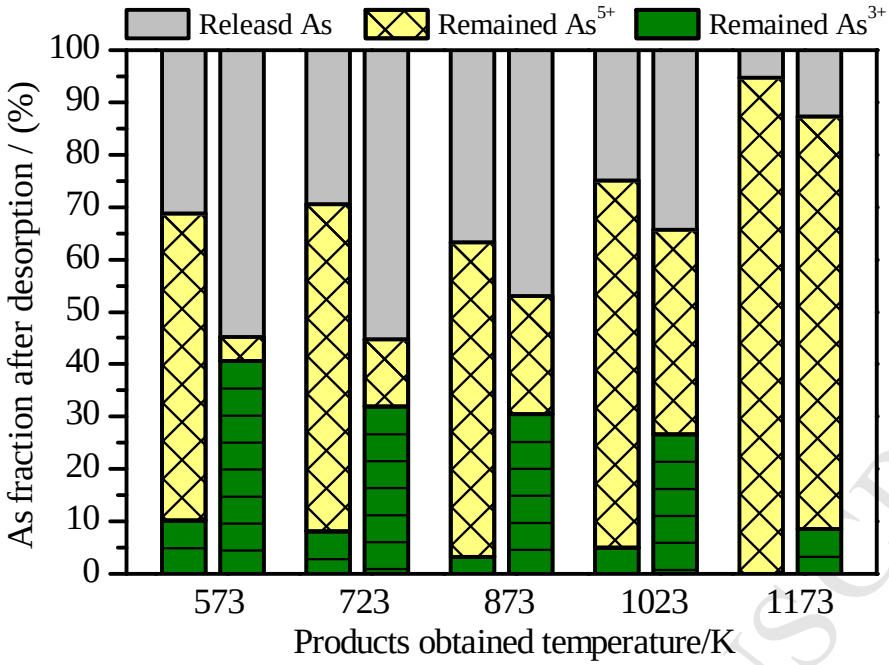

Fig. 4. Arsenic distribution in the reaction products after thermal treatment at 1173 K

(Left column for treatment in air and right column for treatment in N_2)

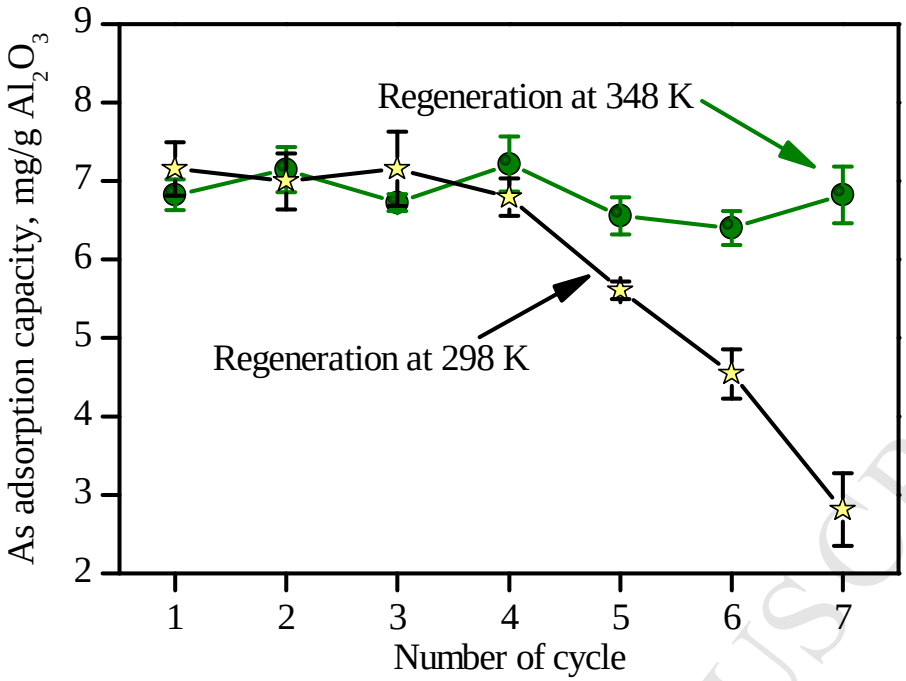

Fig.5. Multiple cycles of arsenic adsorption by alumina regenerated at various temperatures

Highlights

- As capture by γ-Al_2O_3 was effective at a wide temperature range from 573 to 1023 K.
- γ-Al_2O_3 showed good resistance to acid gases in the process for arsenic adsorption.
- As was adsorbed at different active sites in γ-Al_2O_3 by forming various species.
- As capture was inhibited by the change of γ-Al_2O_3 structure at high temperatures.
- The regeneration of spent γ-Al_2O_3 could be well performed using NaOH solution.